

Electrical Resistivity of Undercooled Liquid Cu-Ni Alloys¹

T. Richardsen,² G. Lohöfer,^{2, 3} and I. Egry²

Measured values for the electrical resistivity of undercooled liquid Cu-Ni alloys of different compositions are presented. The experiments were performed in a facility that combines the containerless positioning method of electromagnetic levitation with the contactless inductive resistivity measurement technique. For high nickel concentrations, i.e., for the liquid Cu₂₀Ni₈₀ and Cu₄₀Ni₆₀ alloys, the electrical resistivity shows, as well as for pure nickel and pure copper, the typical linear temperature dependence in the whole range from above to below the liquidus temperature. A significant deviation from the linear behavior occurs for liquid Cu₆₀Ni₄₀ and, less distinct, also for liquid Cu₈₀Ni₂₀. This is explained by a formation of nickel associates in the melt that influence the scattering cross section of the conduction electrons.

KEY WORDS: containerless processing; electrical resistivity; liquid Cu-Ni alloys; short-range atomic ordering; undercooled metallic melt.

1. INTRODUCTION

The temperature-dependent electrical resistivity $\rho(T)$ is an important quantity for the optimal processing of a liquid metal. During casting, or in crystal growth furnaces, ρ controls the melt flow under the influence of electromagnetic fields [1]. For these processes the temperature-dependent thermal conductivity $\lambda(T)$ constitutes another important parameter, because the thermal conductivity controls the heat flow in the melt and has thus a great influence on the solidification process. Direct measurements of this quantity by, e.g., thermal pulse propagation are complicated due to the

¹ Paper presented at the Sixth International Workshop on Subsecond Thermophysics, September 26–28, 2001, Leoben, Austria.

² Institute of Space Simulation, German Aerospace Center, D-51170 Köln, Germany.

³ To whom correspondence should be addressed. E-mail: lohoefer@dv.kp.dlr.de

presence of convective flows. However, λ can be obtained from the electrical resistivity via the Wiedemann–Franz law

$$\frac{\rho(T) \lambda(T)}{T} = L, \quad (1)$$

where the Lorenz number $L = 2.45 \times 10^{-8} \text{ W} \cdot \Omega \cdot \text{K}^{-2}$ is a fundamental constant. Its validity also for liquid metals has experimentally been shown in Ref. 2.

But $\rho(T)$ is also a sensitive indicator for structural changes in the melt. In liquid metals the electrical resistivity results from the scatter of the conduction electrons at the randomly distributed metal ions. It may be expected, that the formation of compact structures (clusters), or a chemical short range ordering of alloy components with decreasing temperature in the melt, should increase the scattering cross section for the electrons and thus also the electrical resistivity. This is opposite to the usually observed linear decrease of this quantity with decreasing temperature, due to the reduction of the temperature-dependent density fluctuations in the melt. Consequently, the onset of ordering phenomena should lead to a deviation of $\rho(T)$ from the typical linear temperature dependence. The lower the temperature of the melt is, the more pronounced this effect should show. This fact makes a measurement of ρ interesting in particular in the undercooled melt, i.e., in the metastable liquid state below the melting temperature T_m .

For undercooled metallic melts, where any mechanical contact with the material causes its immediate nucleation, containerless handling methods of the liquid as well as contactless measurement methods are mandatory [3]. Electromagnetic levitation is an established technique for containerless positioning and heating of metallic melts by means of high frequency alternating magnetic fields [4, 5]. The noncontact measurement of the electrical resistivity of a liquid material can also be based on electromagnetic induction [6–8]. We have combined this measurement technique with the electromagnetic levitation method by placing a pair of measurement coils between the levitation coil [9, 10].

In the following we give a short overview of our measurement technique and show data for the electrical resistivity of liquid Cu-Ni alloys of different compositions.

2. MEASUREMENT TECHNIQUE

Figure 1 shows the arrangement of our measuring transformer between the levitation coils. The alternating current I_1 in the primary coil

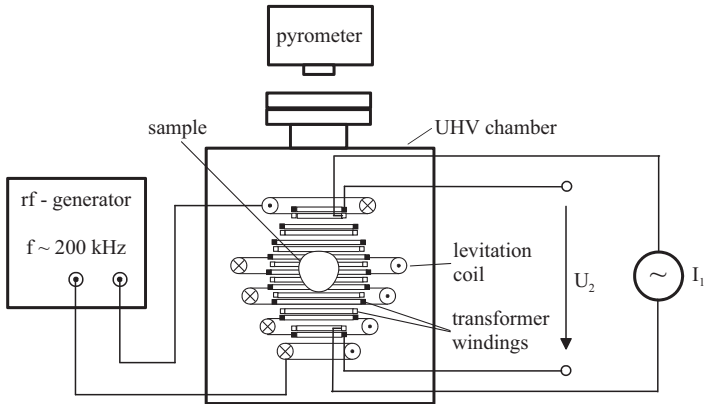


Fig. 1. Schematic diagram of the primary (gray squares) and secondary (black squares) measurement coils integrated with the levitation coil in the UHV chamber.

of the transformer generates a high frequency magnetic field that induces a voltage U_2 in the secondary coil, which depends on the electrical resistivity ρ of the sample, its radius R , and the deviation of its shape from the spherical symmetry α ,

$$U_2 = Z(\rho, R, \alpha) I_1. \quad (2)$$

By a measurement and monitoring of the absolute values of I_1 and U_2 and the phase difference between both, the (complex) impedance $Z(\rho, R, \alpha)$ is determined. In the next step the electrical resistivity of the liquid droplet is calculated from the theoretical relation between Z and ρ , which is well known except for calibration constants that depend on the radius R and the shape factor α . In order to determine these constants, all measurements have to be performed at different current frequencies in the range between 10 kHz and 1 MHz. Furthermore, a calibration experiment with a spherical sample of well defined resistivity and radius has to be carried out.

During the measurement the sample is containerlessly positioned by the levitation field in the center of the measurement transformer. To prevent inductive interactions between the high frequency magnetic levitation field and the measuring coils, the measurement itself is performed only in short time intervals of about 1 ms duration during which the levitation field is completely switched off. Furthermore, to account for drifts in the measurement electronics, some of these time intervals are only used to check the response of the measurement amplifiers on a well defined input signal. More details of the experiment facility can be found in Ref. 9 and especially in Ref. 10.

3. MEASUREMENT PROCEDURE

As sketched in Fig. 1, the assembly of the levitation and measurement coil, in which the sample of 5 mm diameter is processed, is enclosed in an ultrahigh-vacuum chamber. At first, the strong magnetic levitation field is switched on to lift and melt the sample. Then the sample is cooled and undercooled by blowing with a mixture of high purity argon and helium gas. During the cooling phase the sample temperature is kept constant for a while to enable the data acquisition of I_1 and U_2 by a PC.

4. MEASUREMENT RESULTS

4.1. Performance Tests

To check the precision and quality of this facility, we measured first the pure metals copper and nickel. Both materials had a purity of 99.99%. For liquid copper, Fig. 2 shows our experimental data for the electrical resistivity as a function of the temperature above the melting point and in the undercooled regime together with values from the literature [11–13]. Evidently, the absolute values as well as the slope agree to within less

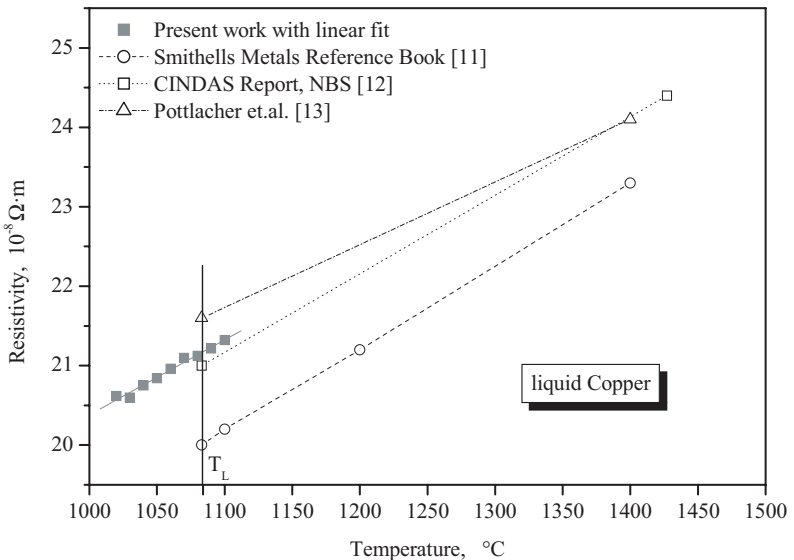


Fig. 2. Electrical resistivity of liquid copper. Measured data from this study (closed squares with linear fit), extending also into the undercooled state below the melting temperature T_L , are compared with literature values (open symbols).

than 5%. All measured data points in the temperature range $1000^{\circ}\text{C} \lesssim T \lesssim 1100^{\circ}\text{C}$ above and below the melting temperature are fitted very well by a typical linear temperature dependence,

$$\rho_{\text{liq. Cu}}(T) = 1.09 \times 10^{-7} + 9.45 \times 10^{-11}T \quad (\Omega \cdot \text{m}) \quad (T \text{ in } ^{\circ}\text{C}). \quad (3)$$

This also means that there is no anomalous behavior of the electrical resistivity when the temperature of the liquid metal passes through the melting point.

This becomes even more distinct for the example of liquid nickel, as shown in Fig. 3. Liquid nickel can, in general, easily be undercooled, because it reacts less to residual oxygen molecules in the process gas atmosphere, which usually trigger nucleation and solidification, than does liquid copper. Here too, all data points in the range $1175^{\circ}\text{C} \lesssim T \lesssim 1475^{\circ}\text{C}$ can very well be fitted with a linear temperature dependence,

$$\rho_{\text{liq. Ni}}(T) = 5.23 \times 10^{-7} + 2.40 \times 10^{-10}T \quad (\Omega \cdot \text{m}) \quad (T \text{ in } ^{\circ}\text{C}). \quad (4)$$

The two data sets in Fig. 3 result from different experiments with different samples and show the typical absolute uncertainty ($< 2\%$) of this

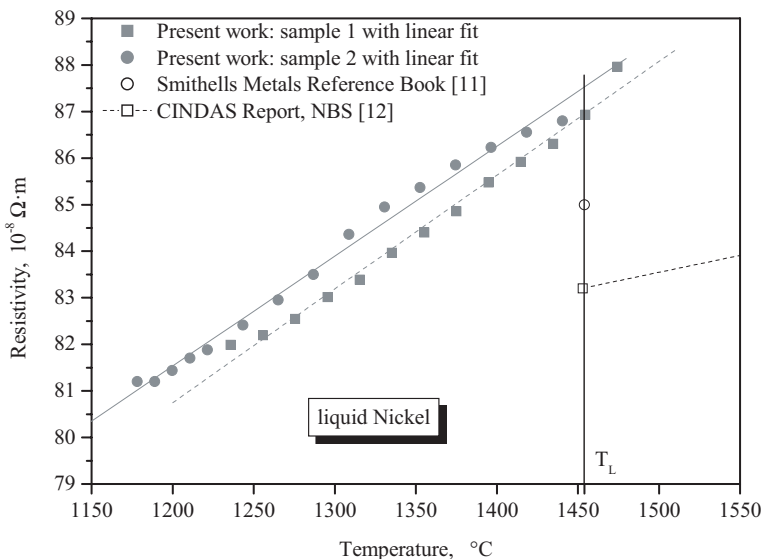


Fig. 3. Electrical resistivity of liquid nickel resulting from two different experiments and samples. Present data (closed symbols with linear fits), extending deeply in the undercooled state, are compared with reference values (open symbols).

measurement facility. As in the case of copper, the literature values of $\rho(T)$ for liquid nickel [11, 12] are smaller than ours.

4.2. Liquid Cu-Ni Alloys

In view of structural changes in metallic melts and their effects on the electrical resistivity, alloys are more interesting than single metals. In single metals only an eventual formation of (icosaedral) atom clusters could have an influence on $\rho(T)$. However, their concentration in the melt is expected to be extremely small [14]. This is different in alloys, where the possible formation of associates (molecules) in the melt at temperatures that can already be reached by undercooling, should lead to a chemical short-range ordering that affects more distinctly the scattering cross section of the conduction electrons and thus also the electrical resistivity.

For measurement of the electrical resistivity of liquid metal alloys, we used Cu-Ni of different concentrations. This material fits to the copper and nickel test samples; it can easily be processed and undercooled in our electromagnetic levitation and measurement facility; it is a very simple and completely miscible system; and finally, this alloy is also of practical interest. Solid $\text{Cu}_{44}\text{Ni}_{56}$, known as constantan in electrical engineering, shows a constant electrical resistivity over a wide temperature range. Figure 4 displays our measured values of $\rho(T)$ for the liquid alloys $\text{Cu}_{20}\text{Ni}_{80}$ and $\text{Cu}_{40}\text{Ni}_{60}$. Over the whole range from about 75°C above to 250°C below the liquidus temperature T_L ($T_L = 1410^\circ\text{C}$ for $\text{Cu}_{20}\text{Ni}_{80}$ and 1347°C for $\text{Cu}_{40}\text{Ni}_{60}$) the electrical resistivity shows the generally expected linear temperature dependence

$$\rho_{\text{liq. Cu}_{20}\text{Ni}_{80}}(T) = 6.49 \times 10^{-7} + 1.59 \times 10^{-10}T \quad (\Omega \cdot \text{m}) \quad (T \text{ in } ^\circ\text{C}), \quad (5)$$

$$\rho_{\text{liq. Cu}_{40}\text{Ni}_{60}}(T) = 6.68 \times 10^{-7} + 1.04 \times 10^{-10}T \quad (\Omega \cdot \text{m}) \quad (T \text{ in } ^\circ\text{C}). \quad (6)$$

However, this behavior changes for lower nickel concentrations. For $\text{Cu}_{60}\text{Ni}_{40}$ the temperature dependence of the electrical resistivity in the liquid state is plotted in Fig. 5. Especially below the liquidus temperature, it becomes evident, that $\rho(T)$ can no longer be fitted by a linear temperature function. The best quadratic fit for temperatures $1100^\circ\text{C} \lesssim T \lesssim 1400^\circ\text{C}$ is given by

$$\rho_{\text{liq. Cu}_{60}\text{Ni}_{40}}(T) = 1.18 \times 10^{-6} - 9.61 \times 10^{-10}T + 4.40 \times 10^{-13}T^2 \quad (\Omega \cdot \text{m}) \quad (T \text{ in } ^\circ\text{C}). \quad (7)$$

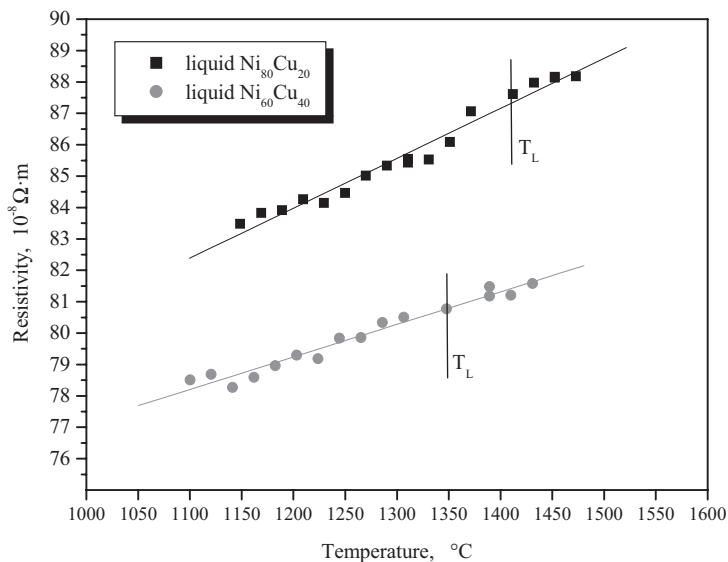


Fig. 4. Electrical resistivity of liquid $Ni_{80}Cu_{20}$ and $Ni_{60}Cu_{40}$ measured above and below the liquidus temperature T_L together with their linear fits.

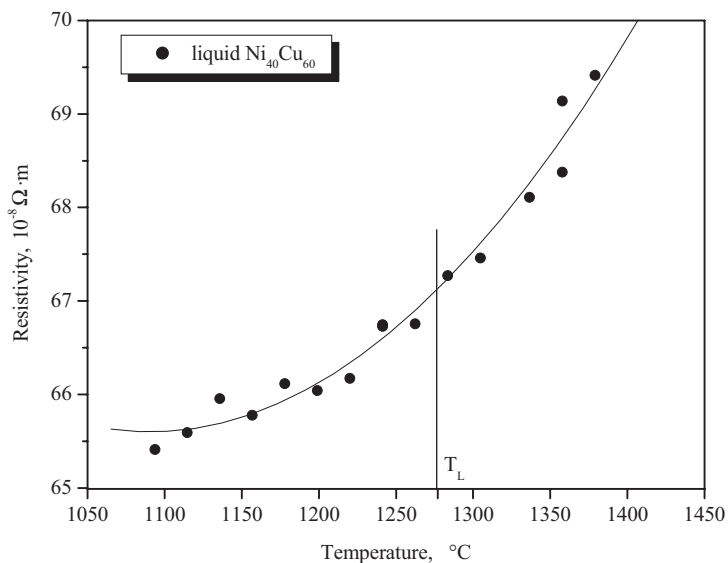


Fig. 5. Electrical resistivity of liquid $Ni_{40}Cu_{60}$ measured above and below the liquidus temperature T_L together with the best quadratic fit. Below T_L , the data show a clear deviation from the typical linear temperature dependence.

The deviation to higher values at reduced temperatures might be explained with a local demixing tendency of the liquid alloy. Since liquid Cu-Ni has a positive mixing enthalpy, which means that heat is required for a mixing of the two alloy components in the liquid state, it may be expected that equal components stay in the mean with decreasing temperature closer and longer together than unequal ones. A close association may be assumed especially for the nickel atoms, which are far below its original melting temperature of 1452°C. This structural chemical ordering in the melt results in local density fluctuations and thus in locally enlarged scattering cross sections for the conduction electrons, which, finally, is the cause for the higher electrical resistivity [15].

For liquid $\text{Cu}_{80}\text{Ni}_{20}$ the temperature dependence of the electrical resistivity, shown in Fig. 6, approaches again the linear behavior of liquid copper. But the quadratic fit,

$$\rho_{\text{liq. Cu}_{80}\text{Ni}_{20}}(T) = 1.13 \times 10^{-6} - 1.29 \times 10^{-9}T + 6.11 \times 10^{-13}T^2 \quad (\Omega \cdot \text{m}) \quad (T \text{ in } ^\circ\text{C}) \quad (8)$$

gives in the temperature range $1100^\circ\text{C} \lesssim T \lesssim 1300^\circ\text{C}$ still a better approximation to the measured values than any linear fit.

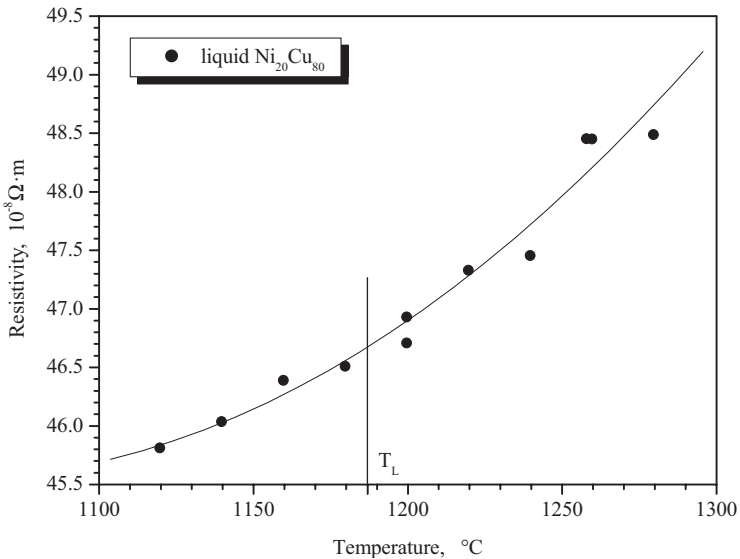


Fig. 6. Electrical resistivity of liquid $\text{Ni}_{20}\text{Cu}_{80}$ measured above and below the liquidus temperature T_L together with the best quadratic fit.

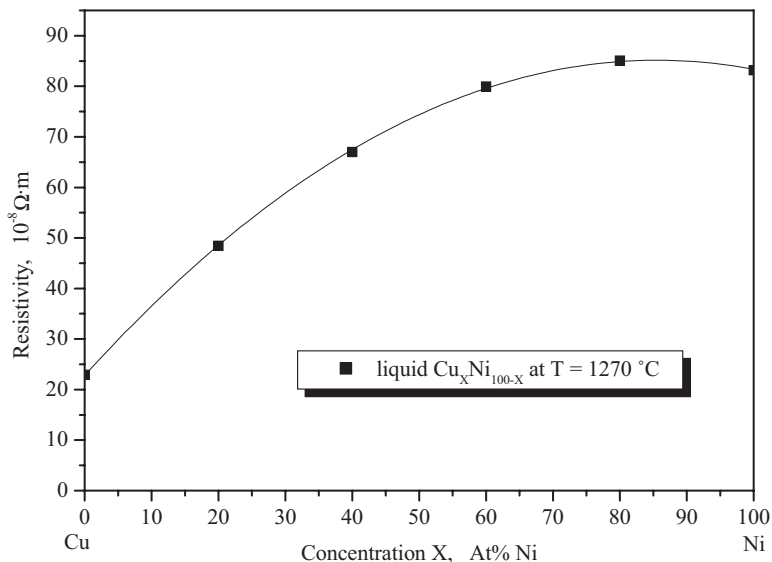


Fig. 7. Electrical resistivity of liquid Cu-Ni at 1270°C as a function of the nickel concentration.

Finally, the electrical resistivity at $T = 1270^\circ\text{C}$ as a function of the compositions of the liquid Cu-Ni alloy is plotted in Fig. 7. The maximum value of ρ occurs near a concentration of 80% nickel atoms.

5. SUMMARY

To determine the electrical resistivity of liquid metals in the undercooled state, we have constructed a facility which combines the containerless electromagnetic levitation technique with the contactless inductive measurement method. As shown in Figs. 2 and 3, the apparatus yields very accurate and reliable results. We then used this facility to measure the electrical resistivity of liquid Cu-Ni alloys of different compositions. For high nickel concentrations, i.e., for $\text{Cu}_{20}\text{Ni}_{80}$ and $\text{Cu}_{40}\text{Ni}_{60}$, as well as for pure nickel, the typical linear temperature dependence is observed in the whole range from above to below the liquidus temperature. A significant deviation from the linear behavior occurs for liquid $\text{Cu}_{60}\text{Ni}_{40}$ and, less distinctly, also for liquid $\text{Cu}_{80}\text{Ni}_{20}$. This is explained by a formation of nickel associates in the melt which increase the scattering cross section for the conduction electrons and thus also the electrical resistivity.

ACKNOWLEDGMENT

The support of this work by the “Deutsche Forschungsgemeinschaft” is gratefully acknowledged.

REFERENCES

1. T. Iida and R. I. L. Guthrie, *The Physical Properties of Liquid Metals* (Clarendon Press, Oxford, 1988).
2. W. Haller, H.-J. Güntherodt, and G. Busch, *Inst. Phys. Conf. Ser.* **30**:207 (1977).
3. I. Egry, G. Lohöfer, and S. Sauerland, *Int. J. Thermophys.* **14**:573 (1993).
4. E. C. Okress, D. M. Wroughton, G. Comenetz, P. H. Brace, and J. C. R. Kelly, *J. Appl. Phys.* **23**:545 (1952).
5. G. Lohöfer, *SIAM J. Appl. Math.* **49**:567 (1989).
6. B. Delley, H. U. Künzi, and H.-J. Güntherodt, *J. Phys. E: Sci. Instrum.* **13**:661 (1980).
7. Ya. A. Kraftmakher, *Meas. Sci. Technol.* **2**:253 (1991).
8. J. E. Enderby, S. Ansell, S. Krishnan, D. L. Price, and M.-L. Saboungi, *Appl. Phys. Lett.* **71**:116 (1997).
9. T. Richardsen and G. Lohöfer, *Int. J. Thermophys.* **20**:1029 (1999).
10. T. Richardsen, *Ein induktives Messverfahren zur Bestimmung der elektrischen Leitfähigkeit an unterkühlten Metallschmelzen* (Ph.D. thesis, RWTH Aachen, 2001).
11. E. A. Brandes and G. B. Brook (eds.), *Smithells Metals Reference Book*, 7th Ed. (Butterworths, London, 1992).
12. C. Y. Ho, M. W. Ackerman, K. Y. Wu, T. N. Havill, R. H. Bogaerd, R. A. Matula, S. G. Ob, and H. M. James, *Electrical Resistivity of Selected Binary Alloy Systems*, CINDAS Report 59 (NBS, Washington, 1981).
13. C. Cagran, A. Seifert, and G. R. Pottlacher, in *Proc. 10th Int. IUPAC Conf. High Temp. Mater. Chem.* (Schriften des Forschungszentrums Jülich, Jülich, 2000).
14. D. A. Porter and K. E. Easterling, *Phase Transformations in Metals and Alloys* (Chapman & Hall, London, 1992).
15. S. Takeuchi and H. Endo, *Trans. JIM* **3**:30 (1962).